Korean J. Chem. Eng., **25**(5), 1145-1150 (2008)

Effects of magnetic field on calcium carbonate precipitation: Ionic and particle mechanisms

Nelson Saksono*, Misri Gozan*, Setijo Bismo*, Elsa Krisanti*, Roekmijati Widaningrum*, and Seung Koo Song,†**

*Department of Chemical Engineering, Faculty of Engineering, University of Indonesia, Kampus UI - Depok 16424, Indonesia
**School of Chemical Engineering, Pusan National University, 30 Jangjeon-dong, Geumjeong-gu, Busan 609-735, Korea
(*Received 2 March 2007 • accepted 27 January 2008*)

Abstract−There are two most widely reported mechanisms to study the effect of magnetic fields on calcium carbonate ($CaCO_3$) precipitate, namely ionic and particle mechanisms. The effects are most debatable because they are contrary to each other. This study explored the effects of both mechanisms in $CaCO_3$ deposit and total $CaCO_3$ precipitation using ionic and particle methods. The ionic method showed reductions in $CaCO_3$ deposit and total precipitation rate of $CaCO_3$, whereas the particle method showed the opposite results. The particle number decreased and the average particle diameter of $CaCO_3$ deposit increased in the ionic method. Meanwhile in the particle method, the particle number increased, average particle diameter decreased and particle aggregation of $CaCO_3$ was observed. XRD measurement on all deposits showed that the crystal deposit was mostly of calcite and the traces of vaterite. However, the amount of the crystal in the particle method was observed to be less than that in the ionic method, indicating that $CaCO_3$ deposit was more amorphous. Particle mechanism decreased the Ca^{2+} ion concentration in solution during magnetization, and ionic mechanism reduced scale ($CaCO_3$) formation after magnetization and separation processes. This method could be applied for decreasing water hardness and prevent the formation of scaling.

Key words: Magnetic Treatment Mechanism, Calcium Carbonate Precipitation, $CaCO_3$ Deposit Morphology

INTRODUCTION

Scale formation, such as on pipe walls and heat exchangers, is a serious problem encountered in almost all water processes. Typical scale deposits are composed of minerals that become less soluble with increasing temperature. Calcium carbonate is the most common deposit. Scale deposits usually form hard-to-remove-linings, which reduce water flow capacities. When they build up on the heat exchanger surfaces, heat transfer efficiency is reduced because of their low thermal conductivity. Anti-scale water treatment using chemical methods changes the solution chemistry and can be very expensive. The chemical methods for water conditioning are economically and ecologically visible especially under conditions of high circulation flow rates for large plants such as thermal power plants. In some other areas, such as food and beverage industries or residential areas, there are strict requirements for water quality. Thus, environmental protection and economic considerations have become strong motivations for developing various types of physical anti-scale methods, among which are ultrasonic, ultraviolet radiation, electric, and magnetic treatments.

The anti-scale magnetic treatment (AMT) of hard waters has been employed for more than a half century. The first commercial device for the treatment was patented in Belgium in 1945 [1]. Powerful electromagnets have been used in hot water systems since the 1960s in the Soviet Union [2]. The application of AMT was first reported in the United States in 1975 [2,3]. In many cases, the magnetic field was delivered by permanent magnets in various geometrical configurations [4]. Several devices were based on alternating current and pulsed fields [5]. According to the review paper of Baker and Judd [4], the efficiency of this treatment is still a controversial question and, as yet, there is no clear explanation of the phenomenon. At the same time, conclusions drawn based on laboratory work sometimes are opposite to each other [4,6].

Two mechanisms have been developed to address magnetic field effects on calcium carbonate precipitation: (1) a direct effect on dissolved ions, and (2) a magnetic effect on particles [7]. The first mechanism is known as the "*ionic mechanism.*" Examples of ionic response to a magnetic field have been reported by Higashitani et al. [8] who investigated the characteristics of calcium carbonate crystals. The crystals were formed by mixing of magnetically treated, quiescent-filtered solutions of calcium chloride and sodium carbonate. At a magnetic flux density greater than 3000 Gauss and exposure times longer than 10 min, it was found that the nucleation of calcium carbonate was suppressed, but the growth of particle size was accelerated and the portion of aragonite particles arose. Higashitani attributes those results mainly to the magnetic exposure of the sodium carbonate solution prior to mixing. Chibowski et al. [9] argued that the hydration energy of an anion CO_3^{2-} is lower than a cation Ca^{2+}. By using spectrophotometer method, Barret and Parsons [10] and Chibowski[a] et al. [9] also found the absorbance reduction, indicating the presence of suppressed nucleation in magnetized solution. Meanwhile, the observation of Kney and Parsons [7] did not notice significant change on the absorbance value of the magnetic solution. Higashitani et al. [11] hypothesized that weak bonds of water molecules with the CO_3^{2-} anion are quasi-stabilized and structured by the magnetic exposure, so that they inhibit the precipitation rate of $CaCO_3$ crystals.

We call the second mechanism, which involves the magnetic effect on existing particles present in water, as the "*particle mecha-*

†To whom correspondence should be addressed.
E-mail: sksong@pusan.ac.kr

nism." Wang et al. [12], using turbidity measurements, observed a faster precipitation and smaller crystals of calcium carbonate in the presence of a magnetic field of up to 8000 Gauss under quiescent condition than in non-magnetic treatment. Lundager Madsen [13, 14] has concluded that the field accelerates the nucleation of sparingly soluble diamagnetic salts of weak acids such as carbonates and phosphates. He suggested that the magnetic field is able to change the orientation of the proton spin and to disturb dehydration phenomenon by hindering the transfer of a proton H^+ from weak acid (HCO_3^-) to a water molecule.

Wang et al. [15], who considered the enhancement of coagulation by a particle alignment, demonstrated the rate increase of aggregation, as determined by weight measurement of sediment from a static solution treated by magnetic fields. Gabrielli et al. [16] have conducted comprehensive experiments in AMT using a calco-carbonic solution in a circulated flowing system. They concluded that the field strength, composition and flow velocity of the solution have significant effects on the scaling rate.

$CaCO_3$ precipitation may occur in aqueous phase and on a surface phase (deposited). Total precipitation of $CaCO_3$ has been widely defined as the total mass of $CaCO_3$ in both phases. In terms of the morphology, $CaCO_3$ particles may be amorphous and polymorphous as crystals of calcite, aragonite and vaterite. Ahn et al. [17], Kobe et al. [18] and Knez et al. [19] using calco-carbonic solution for the investigation of $CaCO_3$ morphology found that there is an increase of aragonite crystals in aqueous phase under magnetic strength above 10 kG. Similar work by Chibowski et al. [20] using solutions of Na_2CO_3 and $CaCl_2$ did not produce significant increase of aragonite in aqueous phase. On the other hand, the morphology of $CaCO_3$ deposit formed by precipitation of $CaCO_3$ on a surface under the influence of magnetic field has not been established and needs to be further investigated because the mechanism of the crystal formation on the surface and in aqueous solution is different [21].

The present study was designed to test and evaluate both mechanisms by examining the amount of $CaCO_3$ deposit formed and the amount of ions Ca^{2+} consumed in solution as a measure of total $CaCO_3$ precipitation both in aqueous solution and on deposit. The morphology of $CaCO_3$ deposit was examined by optical microscope. Their crystal structures were identified by X-ray diffraction.

MATERIALS AND METHODS

1. Water and Electrolytes

Electrolytes $CaCl_2$ and Na_2CO_3 of reagent-grade and deionized water of the resistivity ≅18 MΩ, which was obtained from Milli-Q water system, were utilized. Unfiltered $CaCl_2$ and Na_2CO_3 0.01 M solutions, respectively, were prepared by dissolving each electrolyte into the deionized water, and then kept in airtight bottles at room temperature.

2. Magnetic Field

A static magnetic field was produced by a pair of neodymium magnets fixed to an aluminum frame with the N/S poles 15 mm apart. An average magnetic flux density (B) of 5,200 G was produced, as measured at the center of the two poles with a Hall probe (Hirst GM 04). Each magnet was 100 mm (L)×15 mm (H)×20 mm (W). The distance of the magnetic poles was modified to produce the flux densities (magnetic induction) of 5,200, 4,000, and 2,000 Gauss.

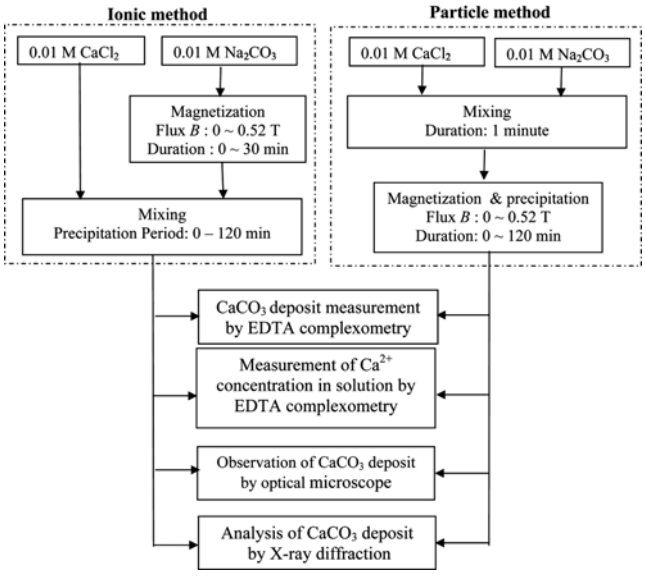

Fig. 1. Experimental method.

3. Experimental Procedure

The experimental method is schematically illustrated in Fig. 1. The experiment consists of two parts. The first part of the experiment used the ionic method. In this method, for each run a magnetic field of a given flux density for a given period of time was exposed to Na_2CO_3 solution in a magnetization tube under the quiescent condition. Most of the solutions, which contained 10 ml of $CaCl_2$ and Na_2CO_3 in 20 ml reactant, were put in precipitation glass reaction tubes (15 mm (OD)×150 mm (H)) right after the completion of magnetic exposure. The wetted surface area on inner wall of glass reaction tube by 20 ml solutions was 5,978 mm^2. The temperature of the solution was not controlled, and equal to the ambient temperature of the surroundings (i.e., room temperature, 28-29 °C).

The second part of experiment used the particle method. In this method, treatment with a magnetic field was conducted during the precipitating process of mixed reactants solution. The $CaCO_3$ deposit formed in the precipitation tube was acquired by removing the solution. The deposit then was dissolved in 20 ml of 0.1 M HCl and its Ca^{2+} concentration was analyzed by EDTA complexometry (accuracy≈0.05 mg as $CaCO_3$). The Ca^{2+} concentration in the removed solution of precipitation tube was also analyzed in the same way. $CaCO_3$ was deposited on a thin-glass that would be used as a sample. The thin-glass sample was vertically dipped into the solution in 30 minutes and the sample object was magnified by microscope optics (Olympus HM 20) and recorded by a camera. The second sample object, which was treated with longer dip (120 minutes), was used to identify the crystal structure of deposit $CaCO_3$ by using X-ray diffraction. The XRD patterns were obtained from Philips PW 1710 using Ni-filtered Cu Kα radiation (λ=0.154184 nm) at 40 kV and 30 mA. The 2θ scanning range was 20-60° with a step size of 0.01° and time per step of 1.0 s.

RESULTS

1. Magnetization Effect on $CaCO_3$ Deposit Formation

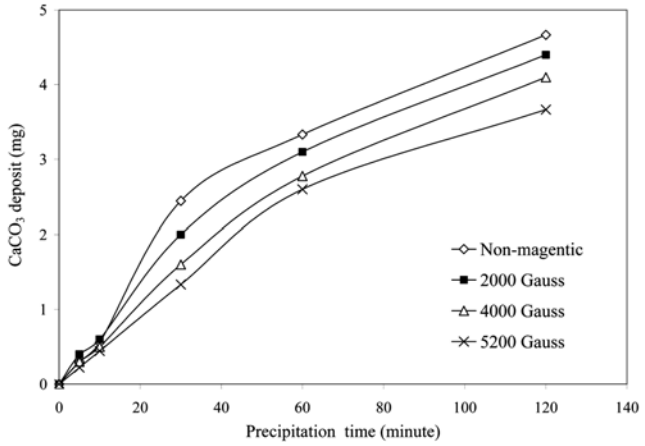

Fig. 2. $CaCO_3$ deposit vs. precipitation time at various flux densities in ionic method. The deposit was observed after the solution had been magnetized for 30 minutes, with deposit surface area 5,978 mm^2.

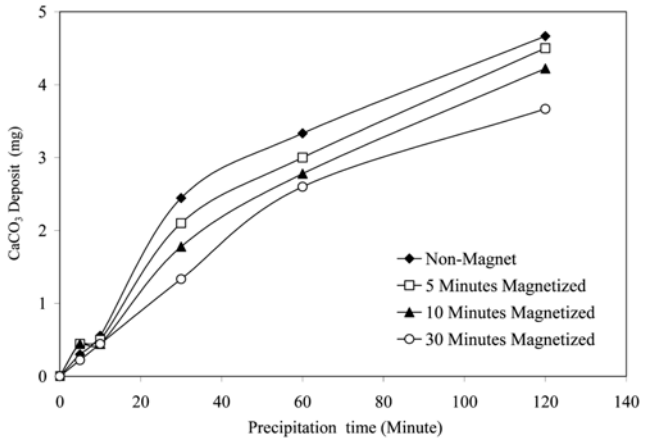

Fig. 3. $CaCO_3$ deposit vs. precipitation time at various durations of magnetization and magnetic flux B=5,200 Gauss in ionic method, with deposit surface area 5,978 mm^2.

Fig. 2 and Fig. 3 show the characteristics of $CaCO_3$ deposit formed on the surface (*heterogeneous precipitations*) under a magnetic field. The amount of $CaCO_3$ deposit increased with the precipitation time. Fig. 2 illustrates the decrease in the rate of $CaCO_3$ deposit formation in the first 30 minutes of precipitation along with the increase in magnetic flux density, and also with the magnetic duration (Fig. 3). The rate of $CaCO_3$ deposit formation after 30 minutes of precipitation of all treatments is approximately constant. This denotes the substantial effect of magnetization occurring only in the first 30 minutes of precipitation. Higashitani et al. [8] found that the optimum magnetic flux and magnetic time in aqueous phase were at 3,000 Gauss and 10 minutes, respectively. This means that our experiments have not reached optimum magnetic flux and magnetic time. This could be due to the difference in $CaCO_3$ precipitation mechanism that occurred in homogeneous and heterogeneous precipitations. With regard to this matter, Ben Amor et al. [22] found that $CaCO_3$ heterogeneous precipitation was predominant compared to $CaCO_3$ homogeneous precipitation, particularly at low hardness condition. However, our study corroborated Higashitani hypothesis

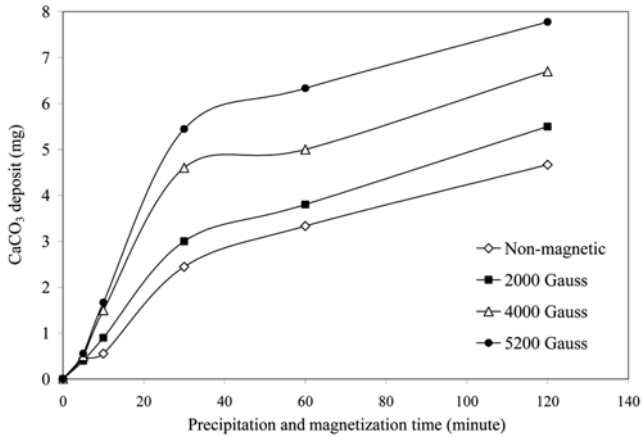

Fig. 4. $CaCO_3$ deposit vs. precipitation and magnetization time at various flux densities in particle method, with deposit surface area 5,978 mm^2.

that the existence of ion hydrate modification by magnetic field retained the nucleation rate.

Particle method results were opposite to the ionic method in terms of the rate of $CaCO_3$ deposition as demonstrated in Fig. 4. There was a significant increase in the rate of $CaCO_3$ deposit as the magnetic flux density increased during the first 30 minutes of precipitation time. The rate of $CaCO_3$ deposit formation after 30 minutes elapsed was almost equal for all treatments although the magnetization was sustained during the precipitation. This indicates the significant effect of magnetization occurring in the first 30 minutes of the precipitation. Wang et al. [15] proposed a correlation inter-particle attraction force for weakly magnetic mineral particles such as $CaCO_3$ as a function of magnetic flux density, distance between particle and particle size.

The difference in the effect of precipitation between ionic solution and particle suspension might be related to the difference in stability of nuclei and ions. During magnetization of Na_2CO_3 solution, the hydrate ion is structured and ion becomes more stable; consequently, this hinders the $CaCO_3$ precipitation after $CaCl_2$ addition. On the contrary, the magnetization on $CaCO_3$ particle suspension increases interaction and attraction forces among particles [12]. This leads to more $CaCO_3$ formation. Furthermore, Lundager Madsen [14] revealed that magnetization of hard water contributed to the transformation of HCO_3^- into CO_3^{2-} which was spontaneously forming $CaCO_3$.

2. Magnetic Effect on Total $CaCO_3$ Precipitation

In the $CaCO_3$ suspension, calcium might be found as $CaCO_3$ deposit, $CaCO_3$ particles in the suspension, and Ca^{2+} ions. The amount of $CaCO_3$ deposit and total $CaCO_3$ precipitation were measured; meanwhile, $CaCO_3$ particles in the suspension were calculated by establishing a material balance. Experimental results on the ionic method (Fig. 5) showed a greater reduction in total $CaCO_3$ precipitation rate in the first 30 minutes of precipitation time by magnetized treatment compared to the rate by non-magnetized treatment. The rate of $CaCO_3$ deposit formation after 30 minutes elapsed almost equally for all treatments. The magnetic flux density also influences the amount of $CaCO_3$ particles formed in ionic method as illustrated in Fig. 5. The trends of the effect of magnetic field on total $CaCO_3$

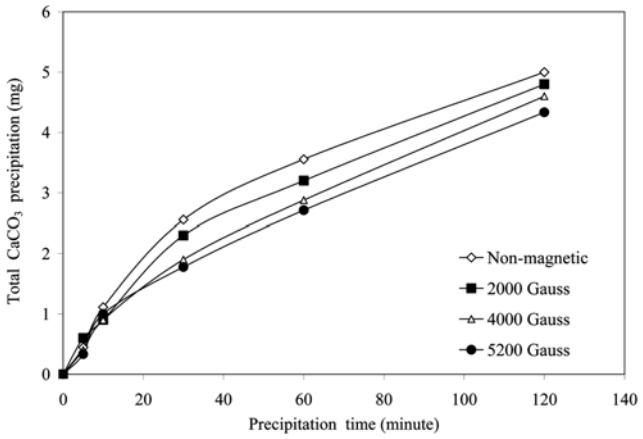

Fig. 5. Total $CaCO_3$ precipitation vs. precipitation time at various flux densities in ionic method. The deposit was observed after the solution had been magnetized for 30 minutes.

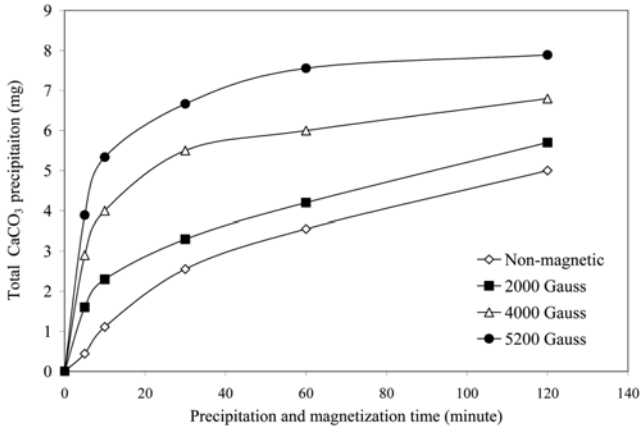

Fig. 6. Total $CaCO_3$ precipitation vs. precipitation and magnetization time at various flux densities in particle method.

precipitation and $CaCO_3$ deposit are similar as demonstrated in Fig. 2 and Fig. 5.

Fig. 6 illustrates the result of the particle method, where the increase in total $CaCO_3$ precipitation rate during the first 10 minutes of precipitation by magnetized treatment is higher than the rate by non-magnetized treatment. The increase of magnetic flux density leads to the increase of the amount of $CaCO_3$ particles. In the same solution model, Barret and Parson [10] also found that the maximum $CaCO_3$ precipitation occurred in the first 9 minutes of precipitation. After 10 minutes of precipitation, the total $CaCO_3$ precipitation rate was relatively constant for all curves. Comparison of the curves correlated between deposit of $CaCO_3$ and total $CaCO_3$ precipitation at different flux densities in ionic mechanism shows that there is similar trend in which the amount of $CaCO_3$ formed is lower as the flux density is increased. Conversely, in the particle mechanism it was observed that the amount of $CaCO_3$ formed was higher as the flux density increased.

There was an interesting result of the particle method as shown in Fig. 7. The amount of $CaCO_3$ particles in solution increased in the first 10 minutes of precipitation time. The amount of $CaCO_3$ particles was greater as the magnetic flux density was increased.

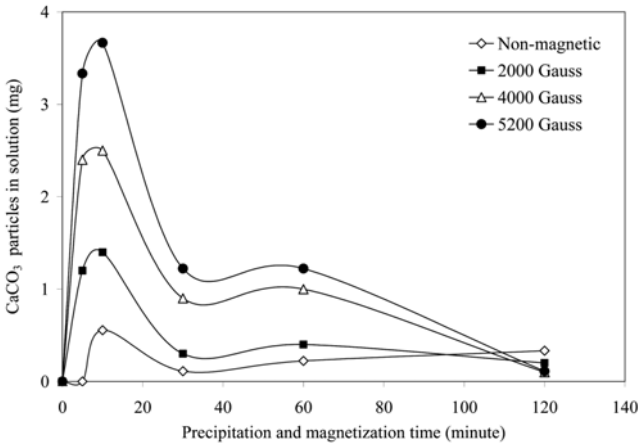

Fig. 7. Amount of $CaCO_3$ particles in solution vs. precipitation and magnetization time at various flux densities in particle method.

This result experimentally upholds the hypothesis given by Wang et al. [12] that a magnetic field enhances the nucleation and aggregation of the $CaCO_3$ in liquid phase. The decreasing amount of particles in solution after 10 minutes of precipitation showed the transformation of $CaCO_3$ particles in liquid phase into the sediments and deposit of $CaCO_3$.

3. Calcium Carbonate Morphology

The morphology of calcium carbonate crystal deposit formed on the surface of the thin-glass sample dipped into the solution was observed with a microscope. It showed that the ionic method by magnetic treatment produced a lower amount of $CaCO_3$ particles compared to the amount by non-magnetic treatment. The particle size by using the ionic method can reach 10 mm. Higashitani et al. [8] found that the average diameter of the particles was greater as the magnetic flux density was increased and as the magnetization time was longer.

On the other hand, the result of the particle method by magnetic treatment (Fig. 8c) showed that the amount of $CaCO_3$ particles was greater compared to the amount by non-magnetic treatment, but the particle size was smaller. Fig. 8c also shows that aggregation occurred in some particles. In general, Fig. 8 shows that some calcite crystals appeared in cubic form.

XRD test result on all the deposit samples as shown in Fig. 9 gives that only one dominant peak appeared at 2θ=29,53°, which indicates that the crystal formed was of $CaCO_3$ calcites. Some infinitesimal peaks were observed at 2θ=26.41°, which indicates that the peaks were of vaterite crystal. This result agrees with the observation by Abdel-Aal et al. [21], who used scanning electron microscopy on the same solution. His observation [21] suggested that the calcite structure dominates the formation of $CaCO_3$ surface crystal. On the other hand, vaterite crystal was not stable phase and would transform to calcite crystal. Vaterite hardly grew on the surface due to its geometric shape. Kobe at al. [18] suggest that the ground electronic state of calcite is much lower than aragonite. Consequently, the Ca^{2+} and CO_3^{2-} ions should have higher kinetic energies to overcome the repulsive forces of the potential barrier in order to form aragonite rather than calcite. Therefore, the formation of calcite is energetically more in favor than that of aragonite.

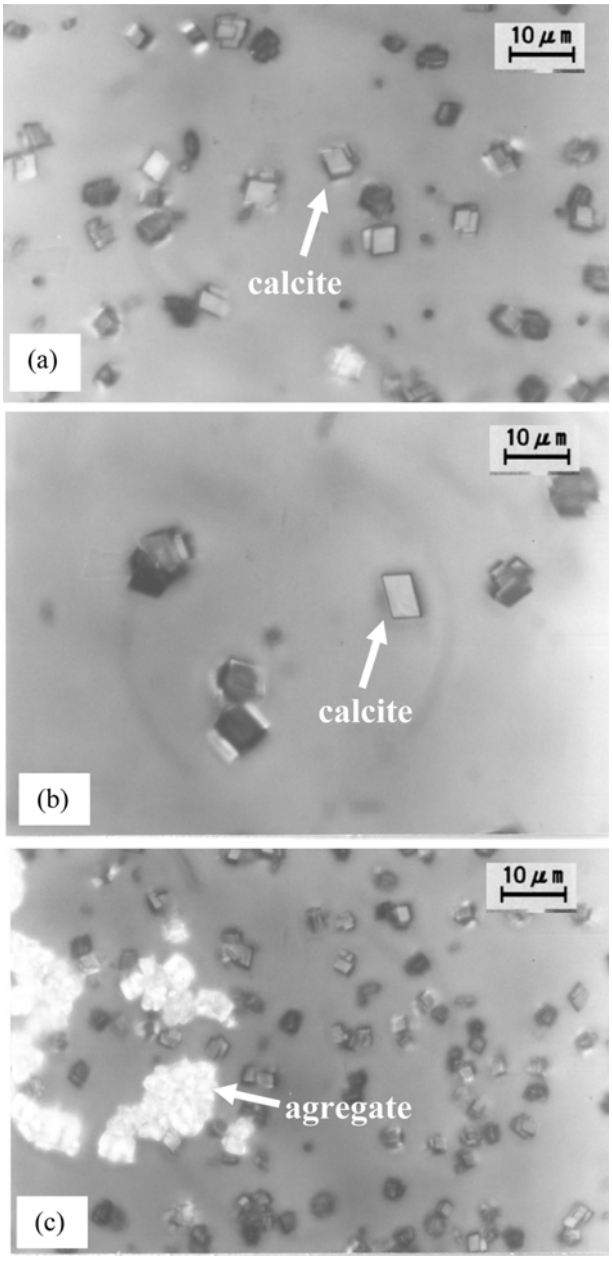

Fig. 8. Images of calcium carbonate crystals deposit at 30 min precipitation: (a) non magnetic treatment, (b) ionic method magnetic treatment, and (c) particle method magnetic treatment.

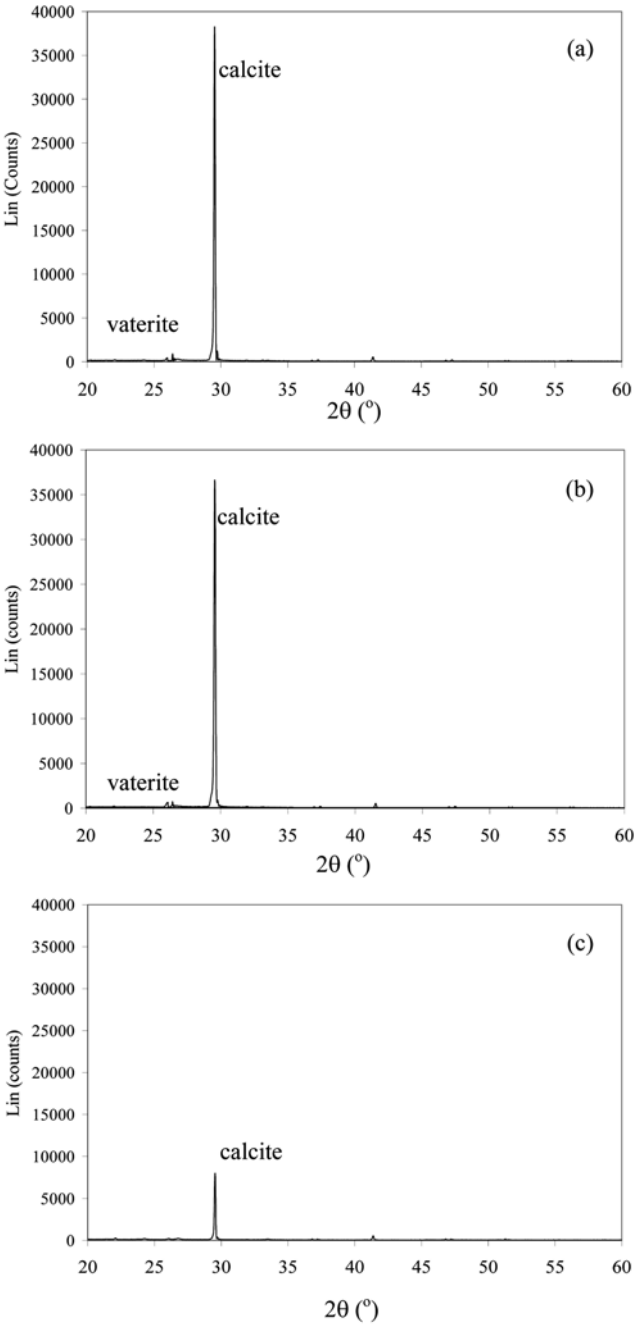

Fig. 9. XRD patterns of calcium carbonate crystals deposit at 120 min precipitation: (a) non magnetic treatment, (b) ionic method magnetic treatment, and (c) particle method magnetic treatment.

Fig. 9 shows the crystallinity of $CaCO_3$ deposit that formed in the particle method by magnetic treatment (Fig. 9c) is lower than that in ionic method by magnetic treatment (Fig. 9b) and that by non-magnetic treatment (Fig. 9a). However, the results of the titration method showed higher deposits. The precipitation, which occurs in particle method, presumably leads to the formation of amorphous calcium carbonate. However, further investigation should be carried out to observe the formation of other crystal forms.

4. Discussion on Anti-scale Magnetic Treatment

The presence of Ca^{2+}, CO_3^{2-} ions, and $CaCO_3$ particles in hard water allows the ionic and particle mechanisms to occur concurrently in the magnetization process. The predominant mechanism depends on the ionic and particle compositions in the solution. Some of researchers, e.g. Higashitani et al. [8], Barret and Parson [10], Chibowski[a] et al. [9], found a memory effect in ionic mechanism in magnetized CO_3^{2-} ionic solution. Therefore, magnetized hard water inhibits the scale ($CaCO_3$) formation even though the magnetic field is removed. The particle mechanism will lead to $CaCO_3$ precipitation and aggregation during magnetization process, thus decreasing the Ca^{2+} ions in the solution.

Another important magnetic effect on $CaCO_3$ precipitation is the

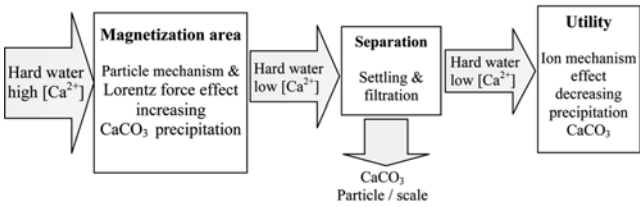

Fig. 10. Anti-scale magnetic treatment in flowing system.

Lorentz force effect. This effect can occur on every ion and charged particle when they are moving through the applied magnetic field (flowing system). Gabrielli et al. [16], Fathi et al. [23], using calco-carbonic solution in a flowing system, found that there is an increase of $CaCO_3$ precipitation rate in solution under a magnetic field. The utilization of a flowing system for AMT application is more effective in terms of capacity and desired effect. Those three effects on the AMT system can be seen in Fig. 10.

The effectiveness of the AMT process is determined by two factors (see Fig. 10), i.e., (1) increasing the amount of $CaCO_3$ precipitation during magnetization by particle mechanism and Lorentz force effects to decrease the Ca^{2+} ion concentration in solution; (2) reducing of scale ($CaCO_3$) formation after magnetization and separation processes, due to ionic mechanism effect on ion hydrate. In the future work, those factors will be used to evaluate the effectiveness of magnetization process with flowing system in order to reach an effective AMT system.

CONCLUSION

This research explains the effect of a magnetic field of $CaCO_3$ deposit and total $CaCO_3$ precipitation, where both were using ionic and particle mechanisms.

Magnetization of ion CO_3^{2-} in solution (ionic mechanism) leads to the decreasing amount of total $CaCO_3$ precipitation and $CaCO_3$ deposit, while magnetization of $CaCO_3$ particle (particle mechanism) leads to the precipitation and aggregation of $CaCO_3$ particles both in solution and on the surface. The magnetic flux density and magnetization time are important variables that influence the $CaCO_3$ precipitation in ionic and particle mechanisms.

The image analysis showed a decreased number of particles and increased particle diameter in the ionic method compared to non-magnetic treatment, whereas in the particle method the trends were in the opposite manner. Calcite was the main crystal identified in $CaCO_3$ deposit. Lesser amount of calcite crystal in the particle method indicates that the $CaCO_3$ deposit was more amorphous. Ionic mechanism, particle mechanism and Lorentz force effects are the main parameters in designing an effective AMT system.

REFERENCES

1. T. Vemeiren, *Corros. Technol.*, **5**, 215 (1958).
2. J. F. Grutsch, *USA/USSR symposium of physical mechanical treatment of wastewaters*, EPA, Cincinnati, 44 (1977).
3. J. F. Grutsch and J. W. McClintock, *Corrosion and deposit control in alkaline cooling water using magnetic water treatment at Amoco's largest refinery*, Corrosion 84 NACE, New Orleans, pp. 330 (1984).
4. J. Baker and S. Judd, *Water Res*., **30**(2), 247 (1996).
5. J. Oshitani, R. Uehara and K. Higashitani, *J. Colloid Interf. Sci.,* **209**, 374 (1999).
6. K. W. Busch, M. A. Busch, D. H. Parker, R. E. Darling and J. L. McAtee Jr., *Corros. NACE*, **42**(4), 211 (1986).
7. A. D. Kney and S. A. Parsons, *Water Res*., **40**, 517 (2006).
8. K. Higashitani, A. Kage, S. Katamura, K. Imai and S. Hatade, *J. Colloid Interf. Sci.*, **156**, 90 (1993).
9. E. Chibowski, L. Holysz, A. Szcześ and M. Chibowski, *Colloid. Surf. A: Physicochem. Eng. Aspects*, **225**, 63 (2003).
10. R. A. Barrett and S. A. Parsons, *Water Res.*, **32**(3), 609 (1998).
11. K. Higashitani and J. Oshitani, *J. Colloid and Interface Science*, **204**, 363 (1998).
12. Y. Wang, A. J. Babchin, L. T. Chernyi, R. S. Chow and R. P. Swatzky, *Water Res.*, **31**(2), 346 (1997).
13. H. E. Lundager Madsen, *J. Cryst. Growth*, **152**, 94 (1995).
14. H. E. Lundager Madsen, *J. Crystal Growth*, **267**, 251 (2004).
15. Y. M. Wang, R. J. Pugh and E. Forssberg, *Colloid Surf. A*, **90**(2-3), 117 (1994).
16. C. Gabrielli, R. Jaouhari, G. Maurin and M. Keddam, *Water Res*., **35**(13), 3249 (2001).
17. J. W. Ahn, J. H. Kim, H. S. Park, S. J. Kim, C. H. Jo and H. Kim, *Korean J. Chem. Eng.*, **22**, 852 (2005).
18. S. Kobe, G. Dražić, A. C. Cefalas and E. Sarantopoulou, *Cryst. Eng.*, **5**, 243 (2002).
19. S. Knez and P. Ciri, *J. Colloid and Interface Science*, **281**, 377 (2005).
20. E. Chibowski, L. Holysz and A. Szczes, *Water Research*, **37**, 4685 (2003).
21. N. Abdel-Aal, K. Satoh and K. Sawada, *J. Crystal Growth*, **245**, 87 (2002).
22. M. Ben Amor, D. Zgolli, M. M. Tlili and A. S. Manzola, *Desalination*, **166**, 79 (2004).
23. A. Fathi, M. Tlili, C. Gabrelli, G. Maurin and M. Ben Amor, *Water Res.*, **40**, 1941 (2006).